

Coupling of lateral and vertical electron motion in $\text{GaAs-Al}_x\text{Ga}_{1-x}\text{As}$ quantum wires and dots

G. Biese, C. Schüller, K. Keller, C. Steinebach, and D. Heitmann
*Institut für Angewandte Physik und Zentrum für Mikrostrukturforschung
 der Universität Hamburg, Jungiusstraße 11, 20355 Hamburg, Germany*

P. Grambow and K. Eberl
Max-Planck-Institut für Festkörperforschung, Heisenbergstraße 1, 70569 Stuttgart, Germany
 (Received 29 November 1995)

Electronic excitations in $\text{Al}_x\text{Ga}_{1-x}\text{As-GaAs}$ quantum wires and quantum dots have been investigated by means of resonant inelastic light scattering. At low frequencies, we find quasi-one-dimensional and quasi-zero-dimensional confined plasmons. Interestingly, we observe, at higher frequencies, not only the original two-dimensional (2D) intersubband excitations, but additional modes ω_k in polarized scattering geometry. The experimental finding is that the frequencies of these modes obey the relation $\omega_k^2 \approx \omega_{2D}^2 + \omega_{1D/0D}^2$, where ω_{2D} is the frequency of the vertical intersubband charge-density excitation. ω_{1D} is a lateral quasi-one-dimensional confined plasmon frequency in wires and ω_{0D} is the frequency of a quasi-zero-dimensional confined plasmon in dots. This relation shows that the additional modes are collective charge-density excitations, which occur due to a coupling of lateral and vertical electron motion.

In recent years, spectroscopic techniques have allowed a deep understanding of the quasi-one-dimensional and quasi-zero-dimensional semiconductor heterostructures. Collective electronic excitations in quantum wires¹⁻⁵ and quantum dots⁶⁻¹⁰ have been observed first by far-infrared transmission spectroscopy. Resonant inelastic light scattering allows the investigation of the wave-vector dispersion of the measured excitations, as well as the distinction between charge-density (CDE), spin-density (SDE), and single-particle excitations (SPE), by means of polarization selection rules.¹¹ Intersubband excitations in quantum wire systems, with many occupied subbands, have been observed first by Weiner *et al.*¹² Egeler *et al.* found an anisotropic plasmon dispersion in multilayered systems, where also many subbands are occupied.¹³ Goñi *et al.*¹⁴ and Schmeller *et al.*¹⁵ investigated one-dimensional intrasubband and intersubband SDE, SPE, and CDE in samples with only two occupied subbands. Very recently, Strenz *et al.* have investigated the wave-vector dispersion of spin-density excitations in quasi-one-dimensional systems, with several occupied subbands.¹⁶ In other samples, they observed confined plasmons.¹⁷ Furthermore, they reported the inelastic light scattering by spin-density excitations in zero-dimensional systems.¹⁶

Starting from single-layered modulation-doped $\text{Al}_x\text{Ga}_{1-x}\text{As-GaAs}$ quantum wells, we have prepared quantum wires and quantum dots by deep mesa etching. It was possible to fabricate structures with lateral size down to 170 nm, which still contain highly mobile electrons. This leads to the unique situation that, in contrast to earlier experiments,¹²⁻¹⁷ we have (a) a huge lateral quantization and (b) the lateral quantization occurs both in the lowest and first excited originally two-dimensional (2D) subband. In our samples, we still have several subbands (in the case of wires) or several electronic levels (in the case of dots) occupied. At low excitation energies, we find several plasmon modes in polarized scattering geometry, which can be fully understood in the picture of confined plasmons.¹⁸ At higher excitation

energies, we observe transitions in the regime of the original 2D intersubband excitations. Interestingly we find, in this regime, additional modes in polarized spectra, which do not exist in the unstructured sample and which we attribute to combined 1D-2D and 0D-2D excitations of collective charge-density type, which occur due to a coupling of lateral and vertical electron motion. We present results, from quantum wire samples, with 500 nm (800 nm) lateral period and 170 nm (270 nm) geometrical wire width and from a quantum dot structure with 800 nm period and 240 nm geometrical dot radius. The samples were prepared by holographic lithography and reactive ion etching. The electron density and mobility of the unstructured 25 nm wide one-sided modulation-doped single quantum well (SQW) at $T=2$ K after illumination were about $8 \times 10^{11} \text{cm}^{-2}$ and $3.5 \times 10^5 \text{cm}^2/\text{Vs}$, respectively. The Raman experiments were performed at $T=12$ K, using a closed cycle cryostat. The energy of the exciting Ti:sapphire laser was in the range of transitions from various confined hole states to the first excited electron state of the unstructured SQW. The power densities were below 10W cm^{-2} . The spectra were analyzed using a triple Raman spectrometer with a multichannel diode array or a liquid nitrogen cooled charge-coupled device camera.

At low excitation energies we observe, in all samples, several plasmon modes in polarized scattering geometry. Figure 1 shows, as an example, the wave-vector dispersion of these modes for the 170 nm wire sample, where the wave-vector q is transferred parallel to the wires. Qualitatively these modes can be understood in the well-known picture of confined plasmons: here, the wave vector q of the 2D intrasubband plasmon has to be replaced by a vector $\{q_{\parallel}^2 + [l(\pi/w)]^2\}^{1/2}$, $l=0,1,2,\dots$, where q_{\parallel} means the wave-vector component along the wires and w is the effective electronic width of the wires. The modes in Fig. 1 are labeled according to the value of l . Quantitatively this simple picture does not hold in most cases.¹⁷ Therefore, the solid

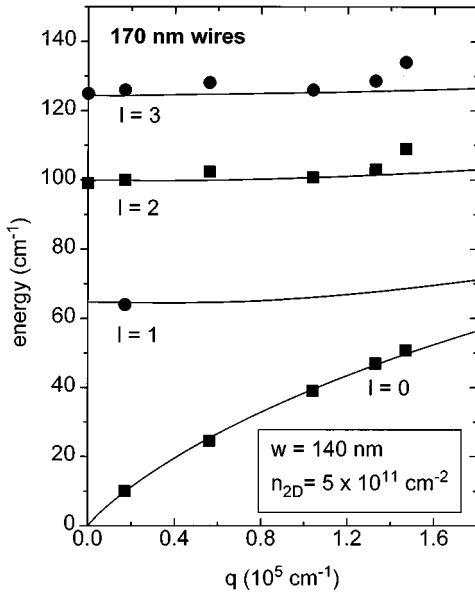


FIG. 1. Wave-vector dispersions of the confined plasmon modes in a 170 nm wire sample. The wave vector q is transferred parallel to the wires. The filled squares mark the symmetric modes and the filled circles the antisymmetric ones. The solid lines are calculated within the hydrodynamical model of Eliasson *et al.* (see text).

lines in Fig. 1 are calculated within the more sophisticated hydrodynamical model of Eliasson *et al.*,¹⁸ which leads in the high wave-vector limit to the above mentioned q dependence of the confined plasmon modes. With an electronic width $w = 140$ nm and an effective 2D carrier density $n_{2D} = 5 \times 10^{11} \text{ cm}^{-2}$, excellent agreement of theory and experimental data is achieved, where no further parameter is required. The symmetric modes with $l=0,2$ are much more prominent in the Raman spectra than the antisymmetric ones with $l=1,3$. This is due to the two-photon nature of the Raman process, in contrast to far-infrared absorption, which is a one-photon process.

At higher frequencies, we observe the originally 2D intersubband excitations, which result from transitions from states $m=0$ to $m=1$, without change in the 1D or 0D quantum number, $\Delta n=0$ (Fig. 2). m is the vertical quantum number. For illustration, we have sketched for the case of wires some single-particle transitions, which contribute to these 2D intersubband excitations in Fig. 3(a) (long arrows). All these transitions sum up and reproduce the originally 2D intersubband excitations. The positions of the 2D intersubband SPE (broad peaks at about 215 cm^{-1} in Fig. 2), CDE (sharp peaks at about 237 cm^{-1}), and SDE (not displayed here) differ only slightly from those in the unstructured sample. Note that the CDE is actually the ω_- mode of the coupled LO-phonon intersubband-plasmon excitations. But there is an additional mode at about 244 (254) cm^{-1} in the 170 (270) nm quantum wire sample and at about 253 cm^{-1} in the dot sample (dark shaded peaks in Fig. 2), which can only be excited in polarized geometry and which does not exist in the unstructured sample. We find that for the wires the polarizations of incident and scattered light can either be parallel (p,p) or perpendicular (s,s) to the wires (Fig. 2). The frequencies of these modes obey the relation $\omega^2 \approx \omega_{2D}^2 + \omega_{1D/0D}^2$, where ω_{2D} is the frequency of the 2D intersubband CDE. We ex-

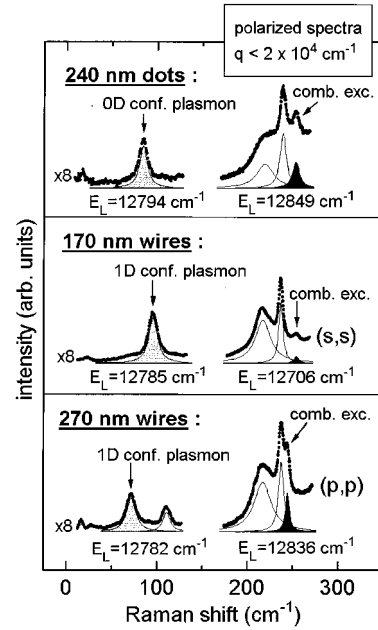


FIG. 2. Polarized spectra for dots and wires. The regimes of confined plasmons and vertical intersubband excitations have been excited with different laser energies for optimum response. The spectra were recorded in quasibackscattering geometry ($q < 2 \times 10^4 \text{ cm}^{-1}$), where the wave-vector transfer and the polarizations of incident and scattered light were either perpendicular (s,s) or parallel (p,p) to the wires in the case of wires, and perpendicular to the sample normal in the case of dots. The broad feature at about 215 cm^{-1} is the 2D SPE and the sharp line at about 237 cm^{-1} is the 2D CDE with $\Delta m=1$ and $\Delta n=0$, where m is the vertical and n the lateral quantum number.

tract from our data that ω_{1D} is actually the frequency of the 2nd lateral confined ($l=2$) quasi-one-dimensional plasmon. ω_{0D} is the corresponding quasi-zero-dimensional confined plasmon frequency. These excitations are most prominent in the Raman spectra, as Fig. 2 shows. The quadratic relation suggests that the additional modes are combined 1D-2D and

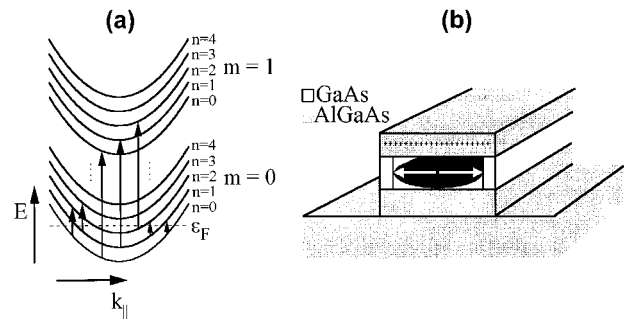


FIG. 3. (a) Sketch of the single-particle transitions, which contribute in quantum wires to the observed intersubband excitations in the regime of the originally 2D excitations (long arrows $\Delta n=0$, $\Delta m=1$) and 1D confined excitations (short arrows with $\Delta n=1$ and $\Delta n=2$). n is the lateral and m the vertical subband quantum number. (b) Schematic picture of lateral (white arrow) and vertical (black arrow) confined electron motion in a quantum wire. The coupling of lateral and vertical collective electron motion results in the experimentally detected combined modes.

0D-2D excitations of the collective charge-density type. The combined excitations occur due to a coupling of lateral and vertical electron motion. In Fig. 3(b), this coupling is visualized in a simple model where the white arrow indicates the lateral and the black arrow the vertical electron motion. The quadratic relation between the energies of the observed modes is surprisingly well fulfilled. This is demonstrated in Fig. 4, where the q dispersions of the relevant modes, the 2nd confined plasmon mode, the 2D intersubband CDE, and the combined mode are displayed for the 170 nm wire and the dot sample. The dotted lines are quadratic polynomial fits to the experimental points. The solid lines are calculated from the dotted ones, according to the quadratic relation $\omega^2 = \omega_{2D}^2 + \omega_{0D/1D}^2$. Furthermore, Fig. 4 shows that the observed excitations in the dot sample are nearly dispersionless compared to those in the wire sample, which is a clear signature of quasi-zero-dimensional behavior. Up to now, the coupling mechanism, which leads to the observed combined modes, is not clear. A coupling between lateral and vertical excitations in three-dimensional quantum dots in tilted magnetic fields was previously observed by Meurer *et al.*¹⁹ In our case, the mechanism may be similar to the coupling of quasi-two-dimensional intra- and intersubband plasmons.^{20,21} However, in the theoretical approach of Das Sarma,²⁰ no additional modes occur, due to the coupling. It will be a task of future work to prove whether or not the combined modes occur, due to the fact that we have, in contrast to quasi-two-dimensional electron systems, a spectrum of several lateral confined plasmons in our quantum wire and dot samples.

In conclusion, we have observed modes in polarized spectra of narrow quantum wire and quantum dot samples, in the regime of the original 2D intersubband excitations. These modes occur, due to the fact that in our deep mesa etched

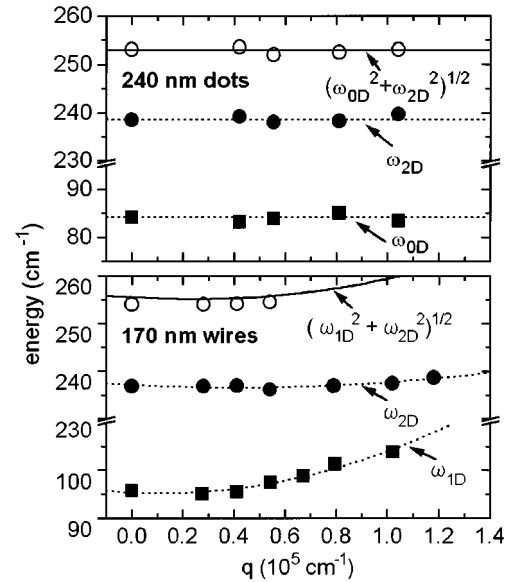


FIG. 4. Wave-vector dispersions of the 2nd confined plasmon frequency, the 2D intersubband CDE, and the combined modes of the 170 nm wire and the dot sample. The dotted curves are fits to the experimental data. The solid lines are calculated from the dotted curves, using the given quadratic relation.

samples, the lateral quantization occurs both in the lowest and first excited originally 2D subband. We show that these modes originate from a coupling of lateral and vertical electron motion, which results in combined 1D-2D intersubband and 0D-2D interlevel excitations of collective charge-density type.

¹W. Hansen, M. Horst, J. P. Kotthaus, U. Merkt, Ch. Sikorski, and K. Ploog, Phys. Rev. Lett. **58**, 2586 (1987).

²F. Brinkop, W. Hansen, J. P. Kotthaus, and K. Ploog, Phys. Rev. B **37**, 6547 (1988).

³T. Demel, D. Heitmann, P. Grambow, and K. Ploog, Phys. Rev. B **38**, 12 372 (1988).

⁴T. Demel, D. Heitmann, P. Grambow, and K. Ploog, Phys. Rev. Lett. **66**, 2657 (1991).

⁵H. Drexler, W. Hansen, J. P. Kotthaus, M. Holland, and S. P. Beaumont, Phys. Rev. B **46**, 12 849 (1992).

⁶M. A. Reed, J. N. Randall, R. J. Aggarwal, R. J. Matyi, T. M. Moore, and A. E. Wetsel, Phys. Rev. Lett. **60**, 535 (1988); W. Hansen, T. P. Smith III, K. Y. Lee, J. A. Brum, C. M. Knoedler, J. M. Hong, and D. P. Kern, *ibid.* **62**, 2168 (1989).

⁷C. Sikorski and U. Merkt, Phys. Rev. Lett. **62**, 2164 (1989).

⁸T. Demel, D. Heitmann, P. Grambow, and K. Ploog, Phys. Rev. Lett. **64**, 788 (1990).

⁹A. Lorke and J. P. Kotthaus, Phys. Rev. Lett. **64**, 2559 (1990).

¹⁰B. Meurer, D. Heitmann, and K. Ploog, Phys. Rev. Lett. **68**, 1371 (1992).

¹¹For an overview, see, A. Pinczuk and G. Abstreiter, in *Light Scattering in Solids V*, edited by M. Cardona and G. Güntherodt, Topics in Applied Physics Vol. 66 (Springer, Berlin,

1988), p. 153.

¹²J. S. Weiner, G. Danan, A. Pinczuk, J. Valladares, L. N. Pfeiffer, and K. W. West, Phys. Rev. Lett. **63**, 1641 (1989).

¹³T. Egeler, G. Abstreiter, G. Weimann, T. Demel, D. Heitmann, P. Grambow, and W. Schlapp, Phys. Rev. Lett. **65**, 1804 (1990).

¹⁴A. R. Goñi, A. Pinczuk, J. S. Weiner, J. S. Calleja, B. S. Dennis, L. N. Pfeiffer, and K. W. West, Phys. Rev. Lett. **67**, 3298 (1991).

¹⁵A. Schmeller, A. R. Goñi, A. Pinczuk, J. S. Weiner, J. S. Calleja, B. S. Dennis, L. N. Pfeiffer, and K. W. West, Phys. Rev. B **49**, 14 778 (1994).

¹⁶R. Strenz, U. Bockelmann, F. Hirler, G. Abstreiter, G. Böhm, and G. Weimann, Phys. Rev. Lett. **73**, 3022 (1994).

¹⁷R. Strenz, V. Roakopf, F. Hirler, G. Abstreiter, G. Böhm, G. Tränkle, and G. Weimann, Semicond. Sci. Technol. **9**, 399 (1994).

¹⁸G. Eliasson, J. Wu, P. Hawrylak, and J. J. Quinn, Solid State Commun. **60**, 41 (1986).

¹⁹B. Meurer, D. Heitmann, and K. Ploog, Phys. Rev. B **48**, 11 488 (1993).

²⁰S. Das Sarma, Phys. Rev. B **29**, 2334 (1984).

²¹S. Oelting, D. Heitmann, and J. P. Kotthaus, Phys. Rev. Lett. **56**, 1846 (1986).